Also AT/20.1.1/052

EFFECTS OF SHADOWING AT THE AT

AT.39.3/006

Jan 07 1991

Ravi

Introduction : Observations with the AT compact array can sometimes involve antenna elemer that are partially shadowed by other antenna elements. Shadowing arises when the array configuration contains closely spaced antennas and the observing declination is low and the hour-angle large. The special problems that can arise during the operation of the array with closely spaced elements are :

(1) Reduction in the effective collecting area of the shadowed antenna.

(2) Correlated response to ground radiation pickup from over-lapping spill-over radiation patterns on the ground.

(3) Correlated response to atmospheric emission from overlapping radiation patterns in the near field of the atmosphere.

(4) Distortion of the radiation pattern of the antenna that has the structure of another antenna in front. Equivalently; this effect can be considered to be diffraction of radiation from the source past the edge of the antenna in front.

(5) Effects due to porosity of the antenna surfaces - radiation incident on the antenna in front leaks through to the antenna behind it.

(6) Effects due to the scattering of radiation off the sub-reflector/feed truss structures and onto the surface of a nearby antenna.

(7) Shift in the effective baseline to the antenna whose aperture is partially blocked.

(8) Changes in the system temperature of the antenna that is shadowed because of the antenna structure in its beam.

Apart from these special effects, the effects of cross-talk (radiation from the electronics at one antenna picked up by a nearby antenna) and external interference are of greater consequence for closely spaced antenna pairs because the fringe rate is reduced. Since the effects of bandwidth and time-averaging smearing are small for short baselines, strong sources (eg. the Sun) far from the region of interest can produce significant responses. This problem can be overcome to a certain extent by adopting larger bandwidth and time-averaging intervals on the short baseline.

Correction for some of the effects of shadowing will vary across the primary beam. Viewed in the sky plane, the primary beam is time-varying due to a varying effective aperture illumination for the shadowed antenna. Equivalently, viewed in the (u,v)-plane, the

measured visibilities are an average over a region of the plane with a weighting (convolving) function that is time-varying. Hence it may be possible to partially correct for these effects only for sources that are small in angular extend as compared to the primary beam size. The corrections could involve (a) increasing the flux on all baselines involving the shadowed antenna by a factor that is inversely dependent on the square root of the effective collecting area, and (b) recomputing the (u,v) coordinates of the visibilities for baselines involving the shadowed antenna.

The hour-angle/declination range over which geometric shadowing occurs is shown in Fig. 1 & 2 for antenna spacings of 30.612 & 61.224 metres respectively. The region to the upper right of the solid curve is not observable due to the elevation limit of 12 degrees for the AT antennas. The region to the lower left is observable; the areas within the central semi-circular regions are observable with shadowing. The contours indicate the degree of shadowing as a ratio of the apparent spacing between the centres of the antennas (as seen from the sky position) to the diameter of each antenna (22 metres). For example, a contour of 0.8 indicates an overlap of (1.0-0.8)x22=4.4 metres between the two antenna apertures as viewed from the sky position (hour-angle & declination) corresponding to the contour point.

Aperture Blockage : The primary effect of shadowing is a reduction in the effective collecting area of the shadowed element. Geometric shadowing will result in a correlated flux density that reduces with the square root of the effective collecting area of the shadowed antenna element. Assuming that the circular aperture of the dish antennas are uniformly illuminated, the normalized correlated flux density in any baseline involving one shadowed antenna is

$$A = \sqrt{1 - \frac{2}{\pi}\cos^{-1} r + \frac{2}{\pi} r (1-r^2)^{1/2}} \quad ; \; r \le 1.$$

r is the ratio of the apparent antenna spacing d (as viewed from the source) to the antenna aperture diameter D. The function is plotted in Fig. 3. Since the ratio (d/D) does not fall below ~0.3 at the AT (Fig. 1), the maximum amplitude decrease expected due to shadowing at the AT is ~40% if only one antenna in the baseline is shadowed and ~65% if both the antennas are shadowed. These expectations assume that (a) the source flux density does not dominate the system temperature, (b) appropriate corrections are made for changes in the system

FIG. 1.

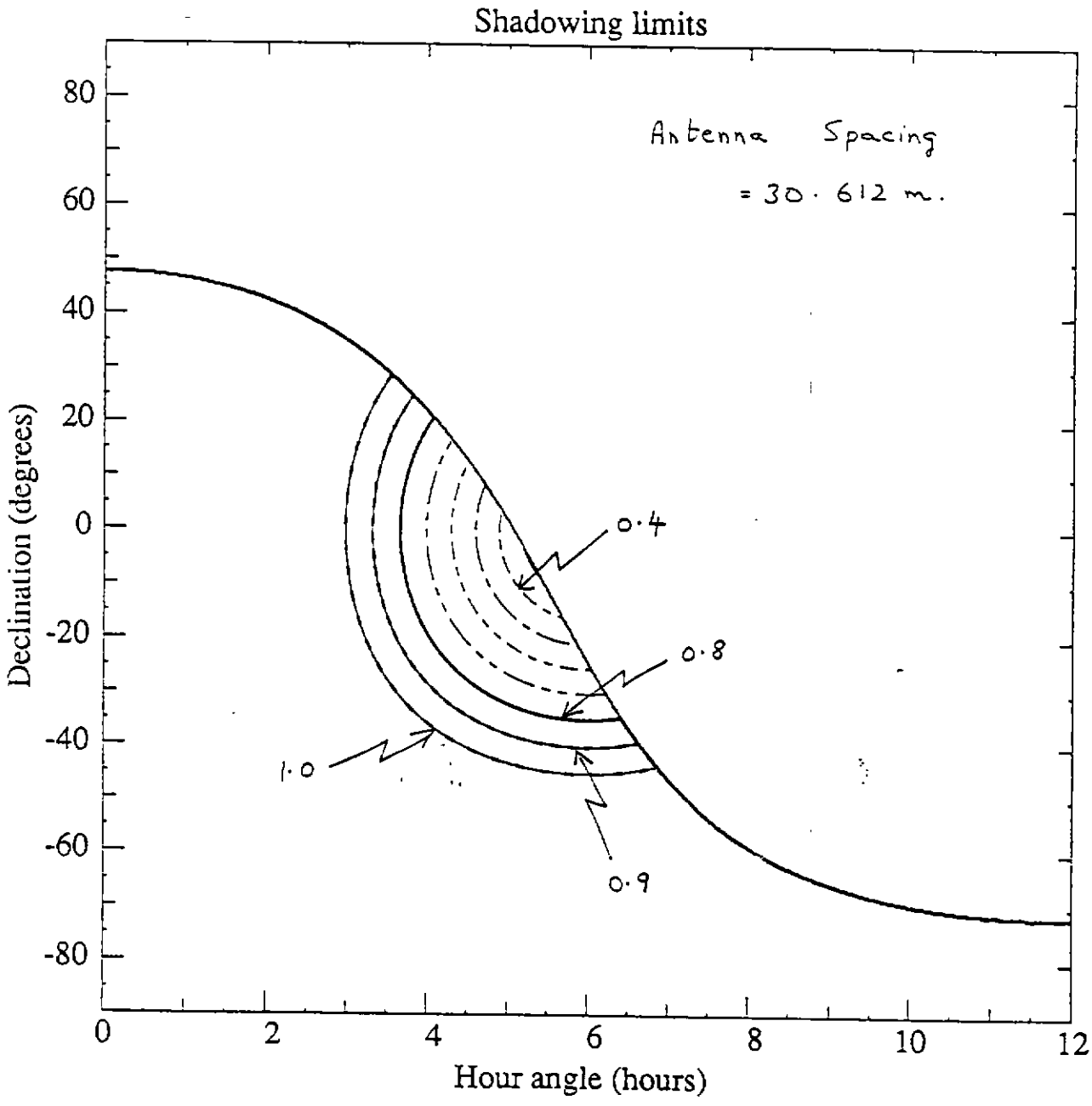
Shadowing limits
Antenna Spacing
= 30·612 m.
0·4
0·8
1·0
0·9
Declination (degrees)
80
60
40
20
0
-20
-40
-60
-80
0
2
4
6
8
10
12
Hour angle (hours)

FIG. 2

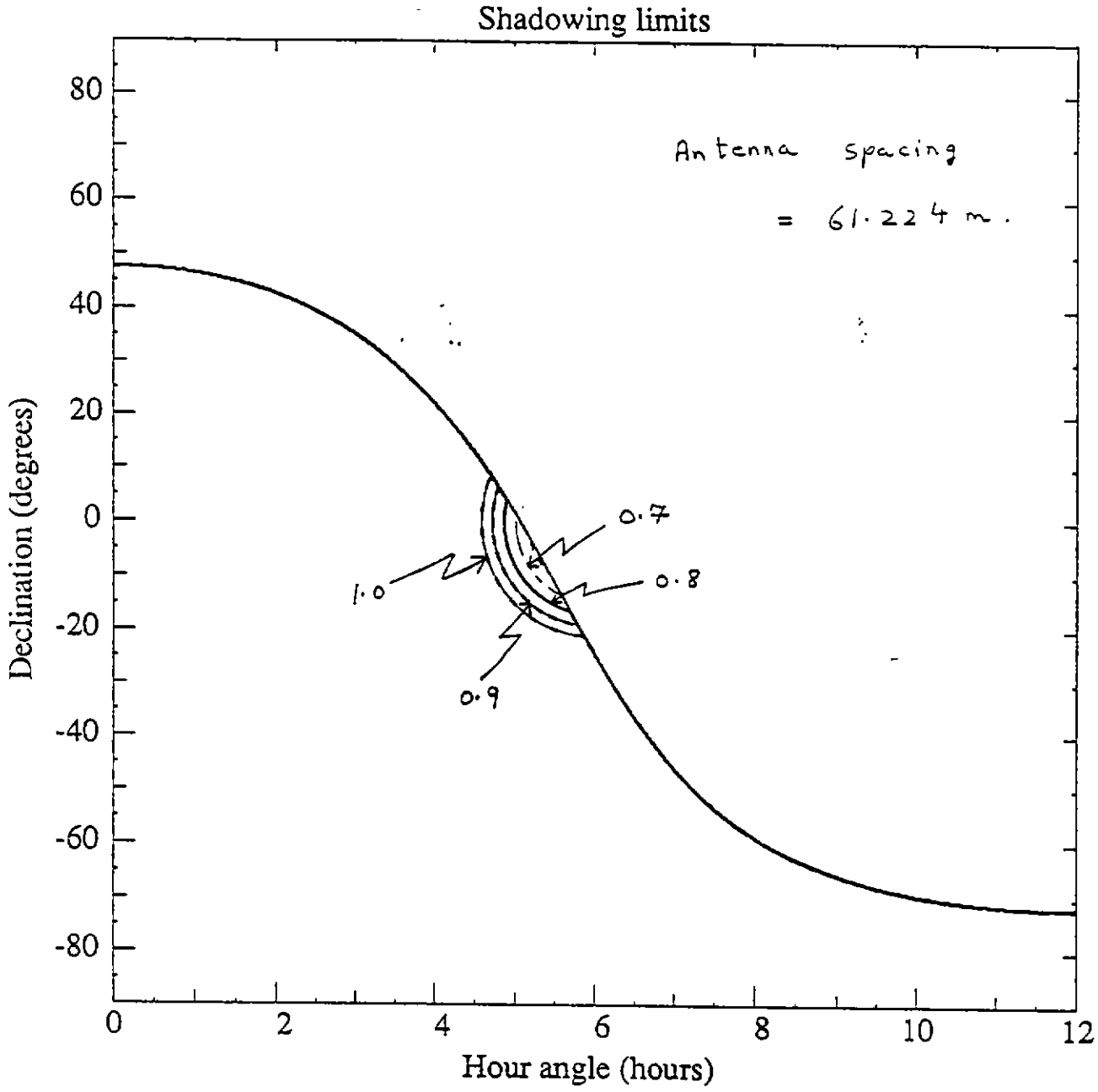
Shadowing limits
Antenna spacing
= 61.224 m.
0.7
0.8
1.0
0.9
Declination (degrees)
80
60
40
20
0
-20
-40
-60
-80
0
2
4
6
8
10
12
Hour angle (hours)

FIG. 3

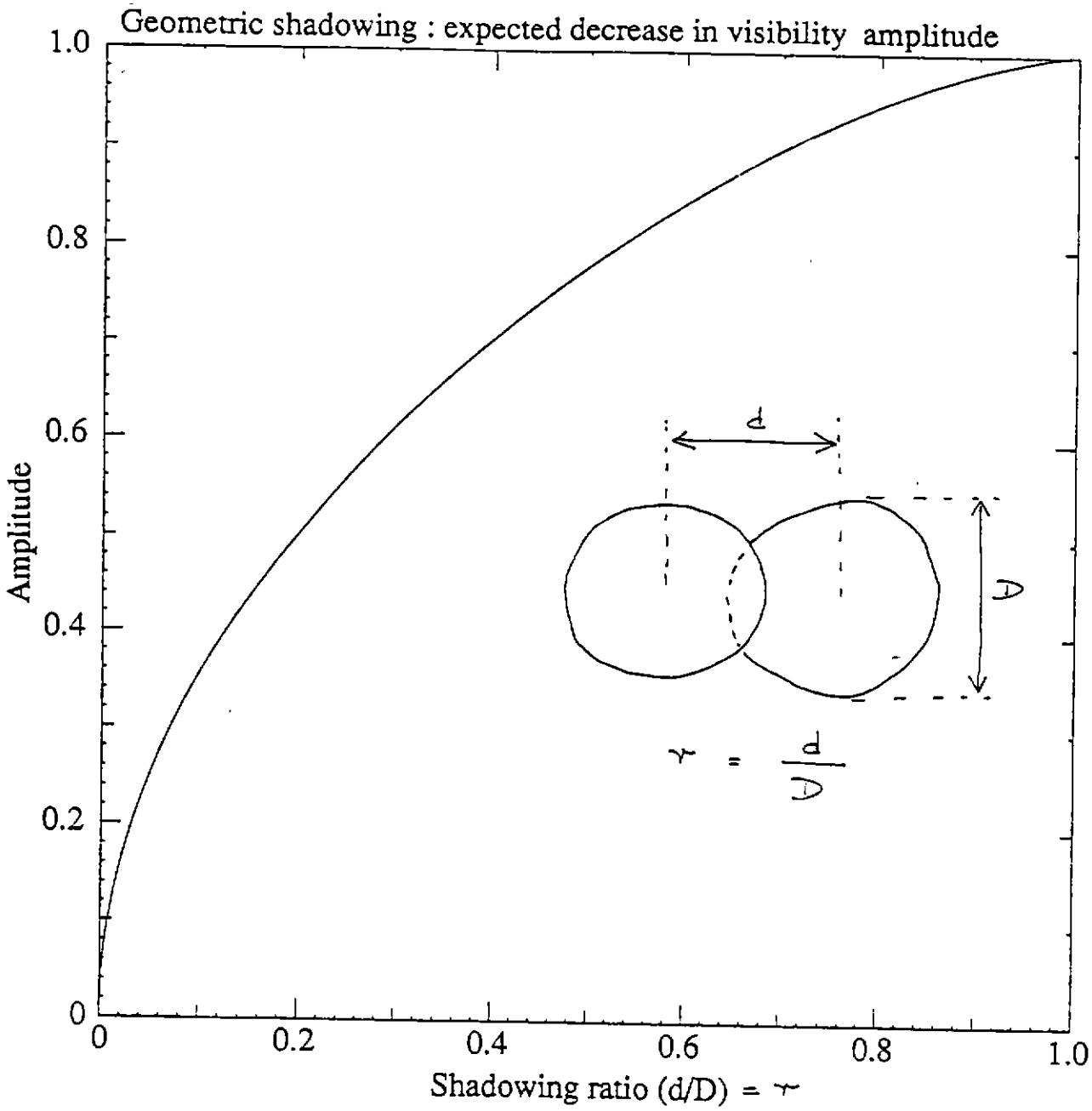
Geometric shadowing : expected decrease in visibility amplitude
Amplitude
1.0
0.8
0.6
0.4
0.2
0
0
0.2
0.4
0.6
0.8
1.0
Shadowing ratio (d/D) = r
d
D
r = d/D

temperature due to variations in elevation angle and due to aperture blockage, (c) the illumination across the aperture is uniform, (d) the source is at the antenna pointing centre and geometric optics is a valid approximation and (e) corrections are made for variations in atmospheric attenuation with varying elevation angles.

Observational results : Unresolved sources located close to 0 degrees declination were observed with three antennas of the AT in a configuration where one baseline was 30.612 m and the other two were several hundred metres. The sources were tracked over an hour angle range where the shadowing parameter r for the 30m baseline decreases progressively from a value above unity to a value below 0.5. The eastern of the two antennas forming the 30m spacing was increasingly shadowed by the antenna to its west as the source set in the west. Plots of the visibility amplitudes in the pair of baselines between the 30m spaced antennas with the third antenna located several hundred metres away were obtained as a function of the projected spacing (or equivalently the shadowing parameter r for the 30m spacing). The amplitudes are an average over the central 50% of the band. The baseline with the western of the 30m spaced antennas forms a reference for the baseline with the eastern antenna which is exected to show the effects of shadowing. Figs.4 to 7 show the amplitude plots for frequencies in the four operational bands of the AT.

The reference baseline does not have a constant amplitude although the on-line system temperature corrections had been applied. The variations are worse in the L/S bands where the rise in amplitude is as much as ~25%. This is indicative of non-linearity in the system temperature measuring machinery. The variations in system temperature are expected to be different in the two antennas forming the 30m baseline and hence it is not clear that the reference baseline amplitude can be used to calibrate the baseline that shows the effects of shadowing.

The baselines with the shadowed antenna show an amplitude reduction in all the four bands. In Table 1 we give the amplitude counts on the reference and shadowed baselines at r=1 & 0.5 (r is computed for the 30m spacing) and compute the fractional reduction in the shadowed baseline at r=0.5. The result of correcting this fractional reduction with the observed reduction in the reference baseline is also shown. The expected reduction is 0.78 and clearly, the observed amplitude falls off more sharply. This could be due to a non-uniform illumination.

Fig 4 (a)

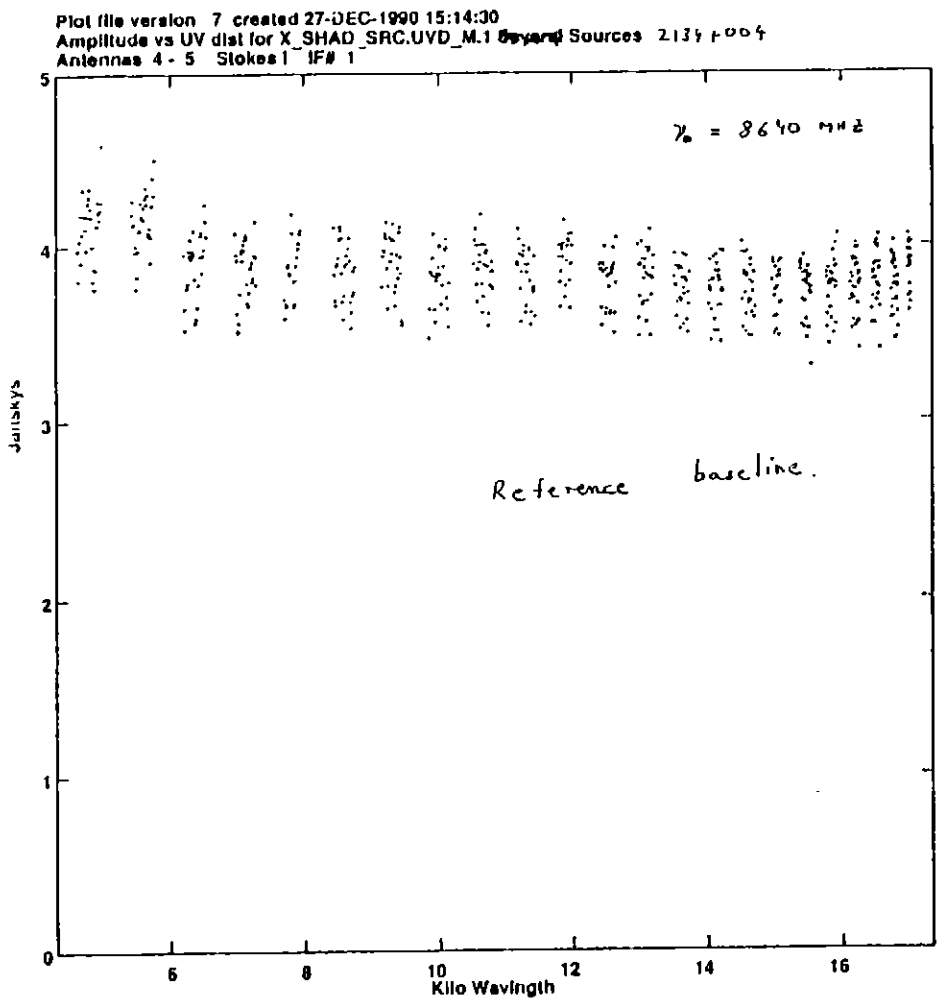

Fig 4 (b)

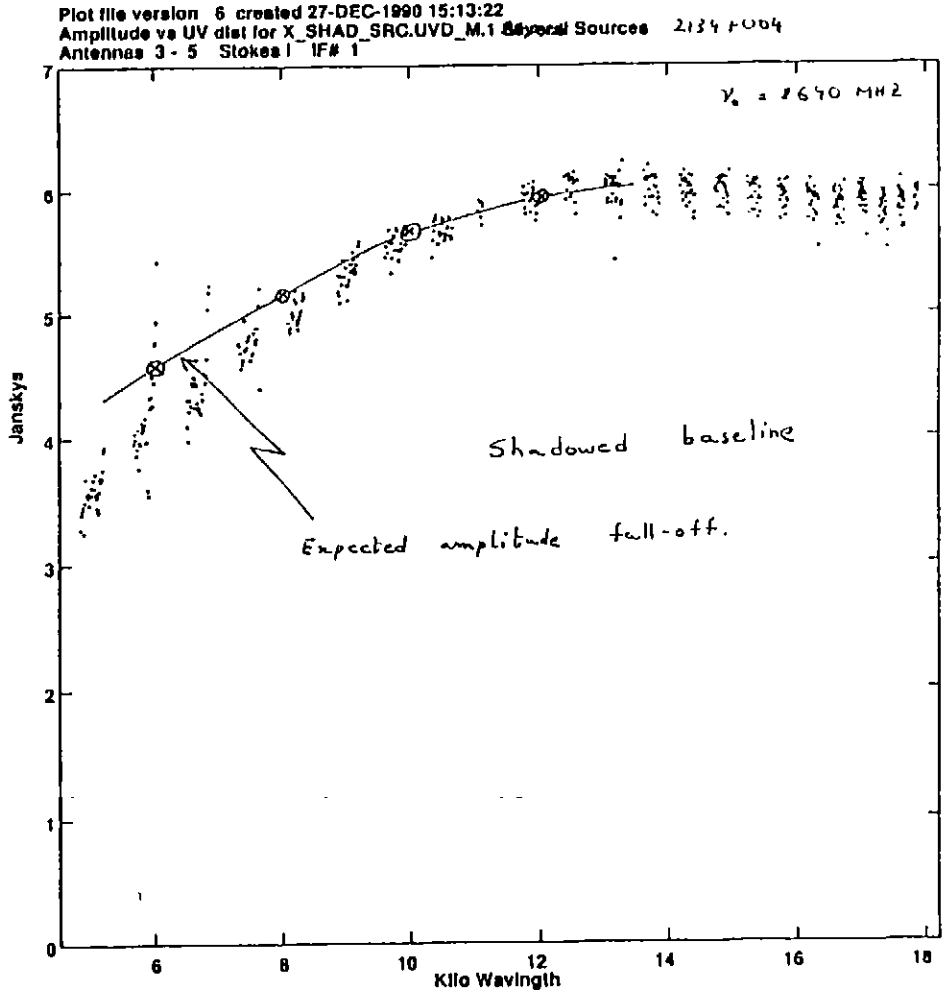

0.47 0.63 0.79 0.95 1.10 1.26 1.42

$\tau \longrightarrow$

Fig. 5 (a)

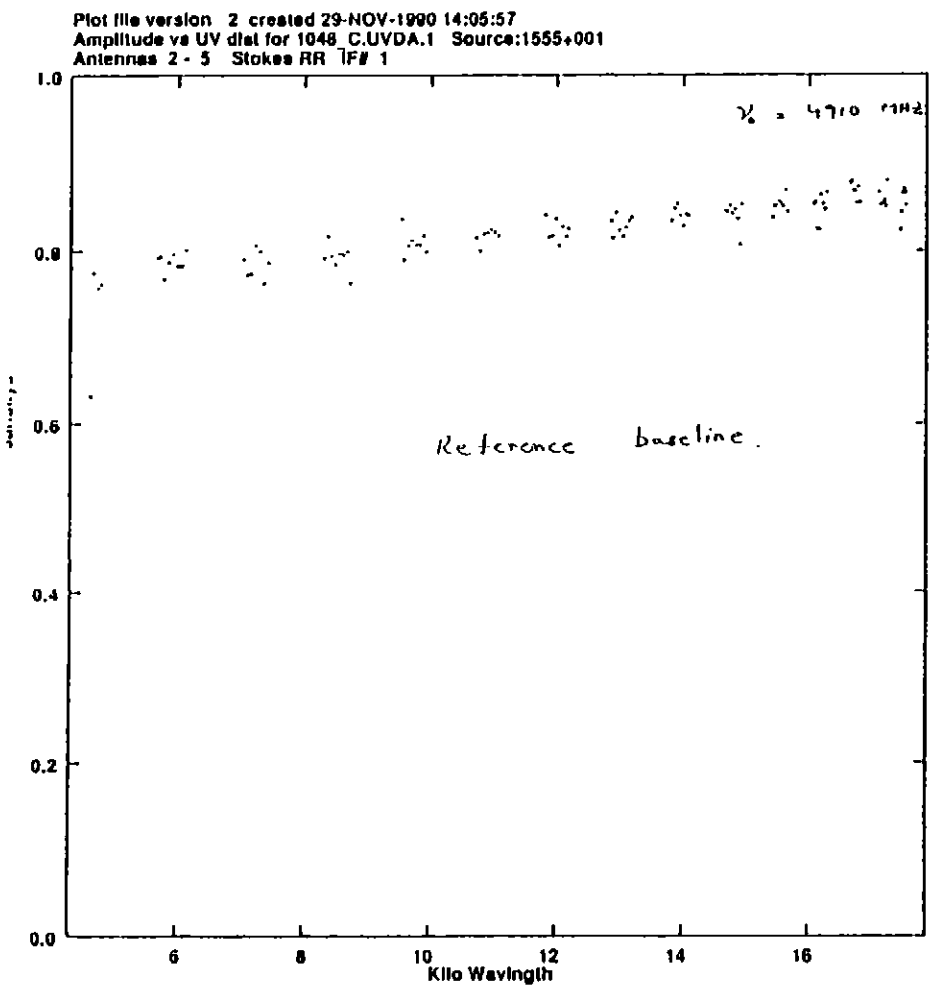

Fig 5 (b)

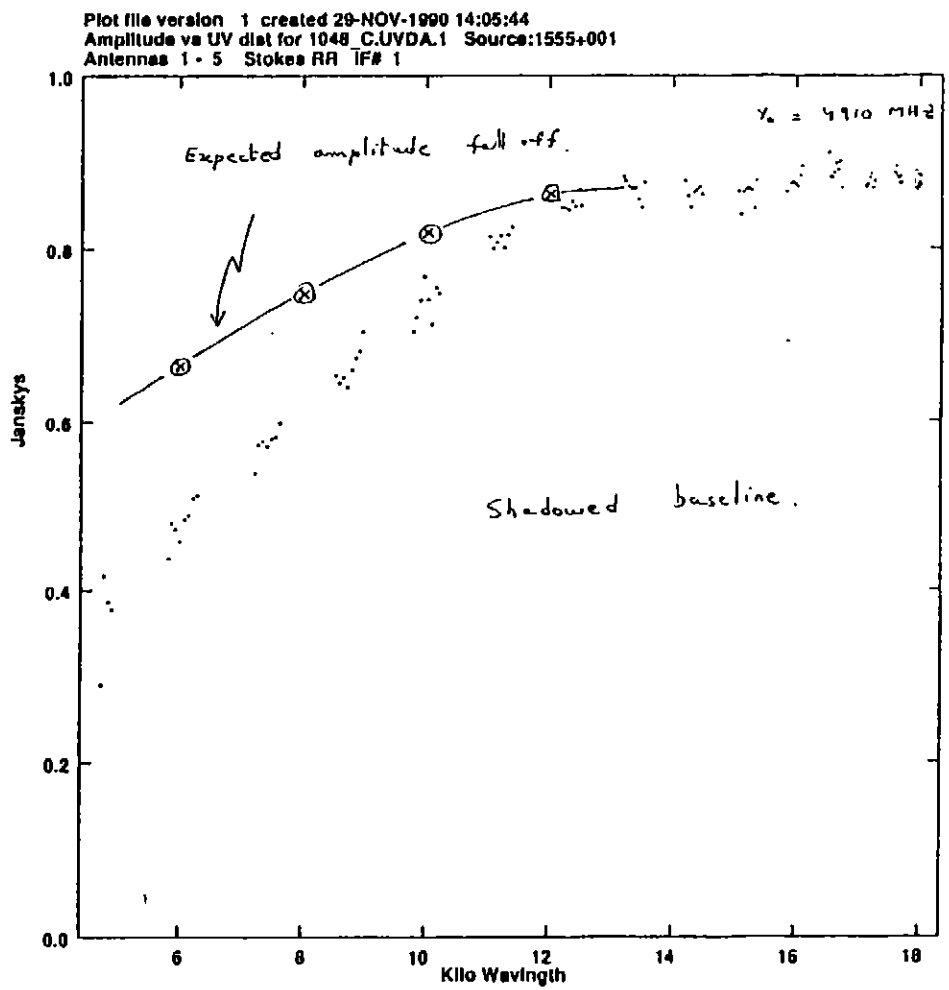

0·47 0·63 0·79 0·94 1·10 1·26 1·12

$r \longrightarrow$

Fig 6 (a)

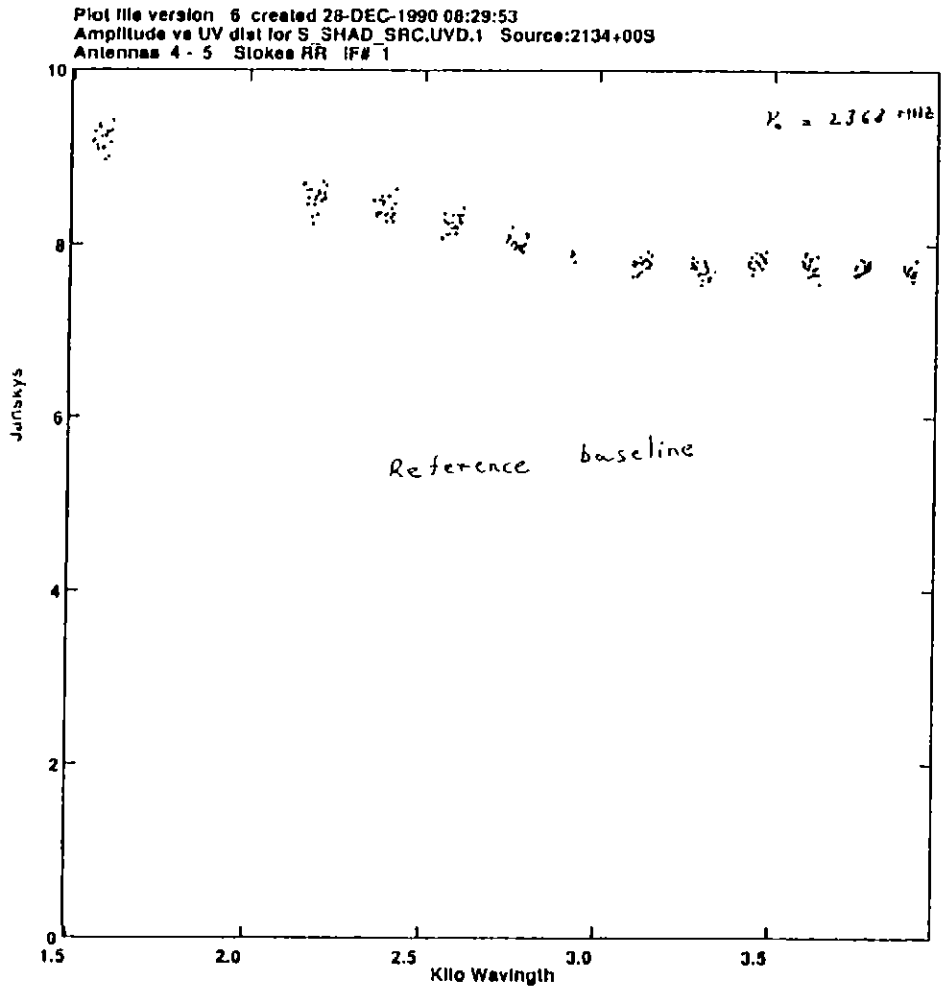

Fig 6 (b)

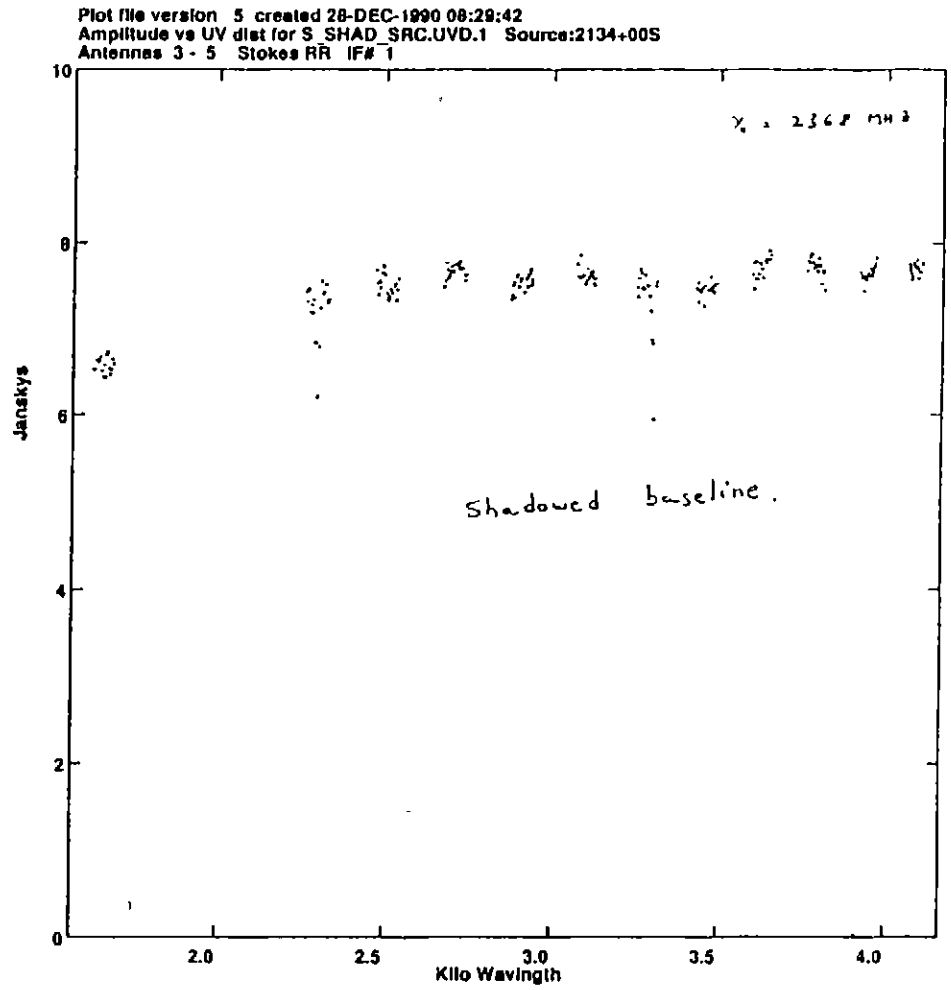

0.58 0.72 0.86 1.01 1.15

τ ⟶

Fig 7 (a)

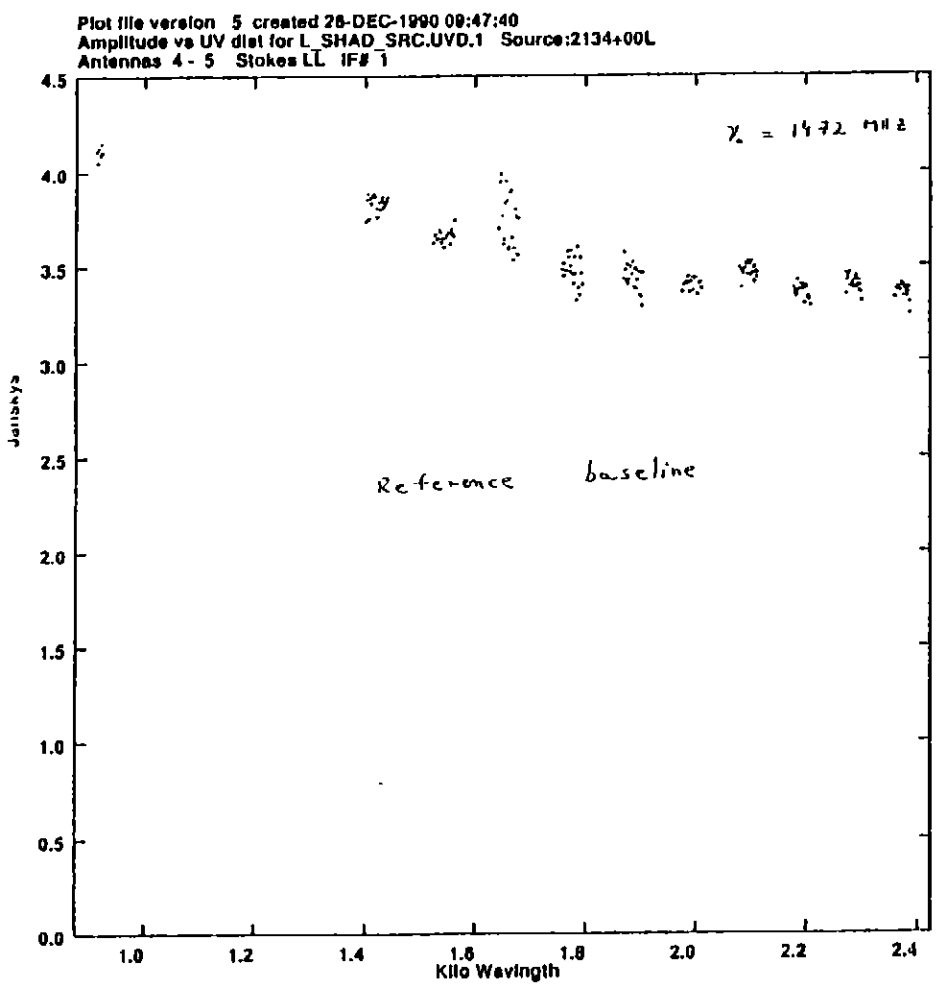

Fig. 7 (b)

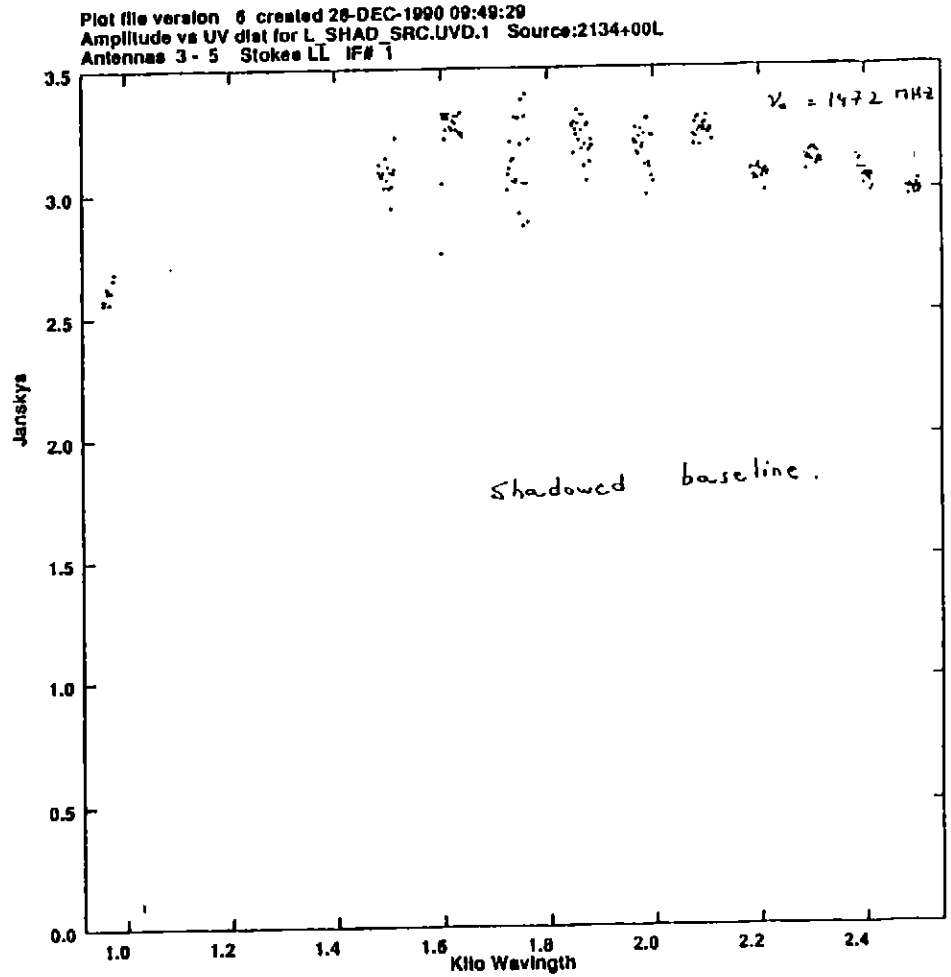

0·46 0·56 0·65 0·74 0·83 0·93 1·02 1·11

$r \longrightarrow$

Table 1

Freq (MHz)	Observed amplitudes				Amplitude ratio	
	Ref. bsln.		Shad. bsln.		Shad. bsln.	Calibrated
	r=1	r=0.5	r=1	r=0.5		
8640	3.7	4.0	6.0	4.2	0.70	0.65
4910	0.83	0.78	0.87	0.51	0.59	0.62
2368	7.7	9.1	7.5	6.7	0.89	0.75
1472	3.4	4.0	3.2	2.7	0.85	0.71

Amplitudes on the 30m baseline : We now consider the visibilities on the 30m baseline, where problems arising from proximity in the antenna elements can occur.

(i) L-band : The amplitudes in XX & YY polarizations show neither a decrease (as seen in longer baselines involving a shadowed antenna) nor an increase (as seen in longer baselines that do not involve any shadowed antenna). This suggests that as shadowing sets in there is an increasing amount of spurious correlation (about 1 Jy ar r=0.5) in this baseline. With r decreasing below unity, the amplitudes of the XY & YX cross-polarizations also rise to a value of about 0.6 Jy at r=0.5.

(ii) S-band : The XX & YY cross polarizations show a rise in amplitude with decreasing r and suggest spurious correlation at the few Jy level at r=0.5. The XY & YX cross-polarizations also show spurious correlation following the onset of shadowing that rises to a value of about 1 Jy at r=0.5.

These experiments in the L/S bands were performed on a VLA calibrator (2134+004) that is considered to be a good amplitude calibrator (<5% extension at 20 & 6 cm in all four VLA array configurations).

(iii) C/X-bands : The VLA calibrator 1555+001 (<10% extended at 2cm in all the VLA configs., <5% extended at 6cm in all the VLA configs.) was tracked down to the western elevation limit with a 30m baseline of the AT. The observing frequency was alternately switched between the C &X bands. The observed correlated amplitudes in XX, YY, XY & YX cross-polarizations are shown in Fig. 8 as a function of time. The shadowing parameter r=1 at 1315 UT and r=0.5 at 1500 UT.

Spurious correlated signal is seen in both C & X bands for r<1. At r=0.5, this signal is at the level of 0.5 Jy in C & X bands. The spurious signal has a high percentage linear polarization (the % polarization is greater in X-band). In all the cross-products, the spurious signal is

Fig. 8 (a)

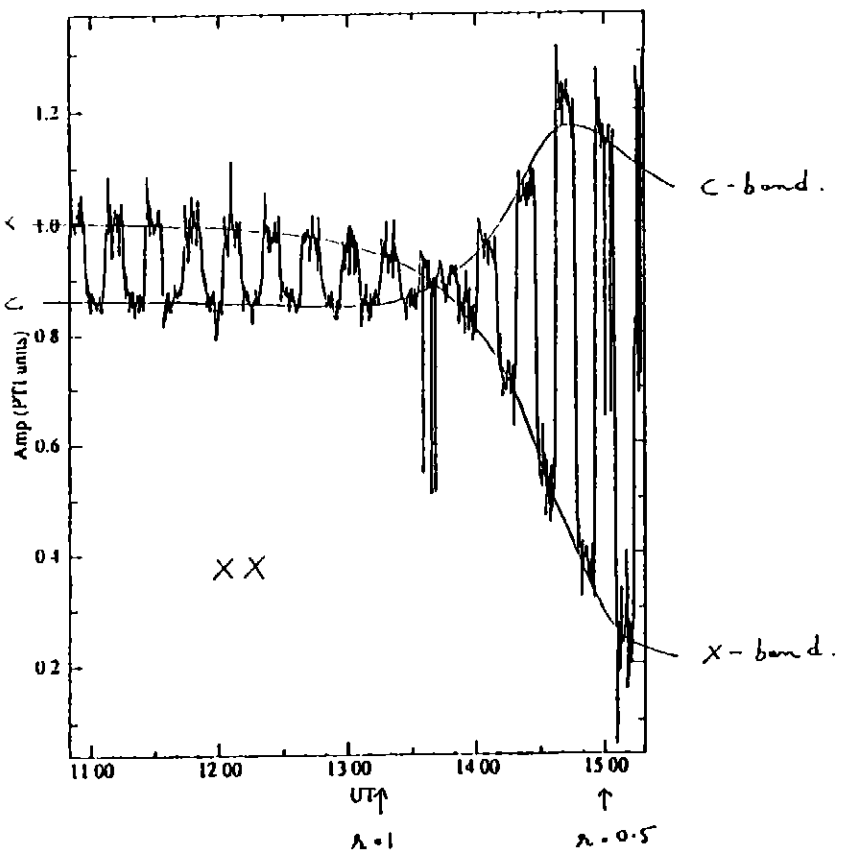

file : CUL2:[OBSERVER.DAT]90-07-17_1048.RPF
Channel id : 8-24 I BA21 buff 1
sources :
1555+001
file : CUL2:[OBSERVER.DAT]90-07-17_1048.RPF
Plotted on 18-JUL-90 at 22:10:58
Frequency: 8740.00 MHz
See pti$tmp:plt.lis for a statistical summary

Fig 8 (b)

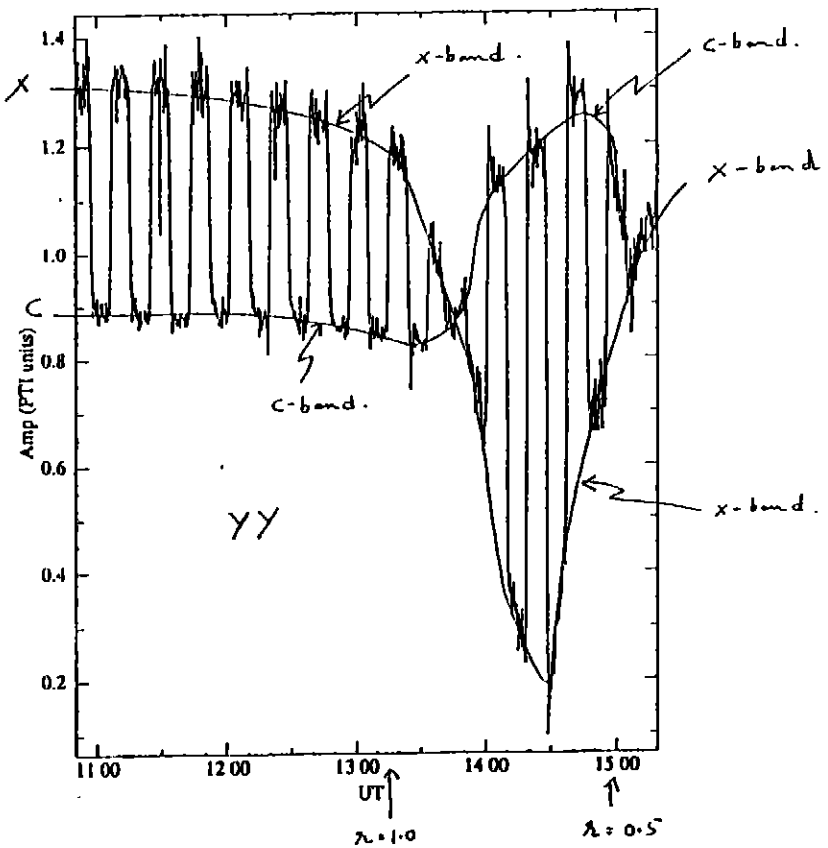

file : CUL2:[OBSERVER.DAT]90-07-17_1048.RPF
Channel id : 8-24 Q BA21 buff 2
sources :
1555+001
file : CUL2:[OBSERVER.DAT]90-07-17_1048.RPF
Plotted on 18-JUL-90 at 22:11:18
Frequency: 8740.00 MHz
See pti$tmp:plt.lis for a statistical summary

Fig 8 (a)

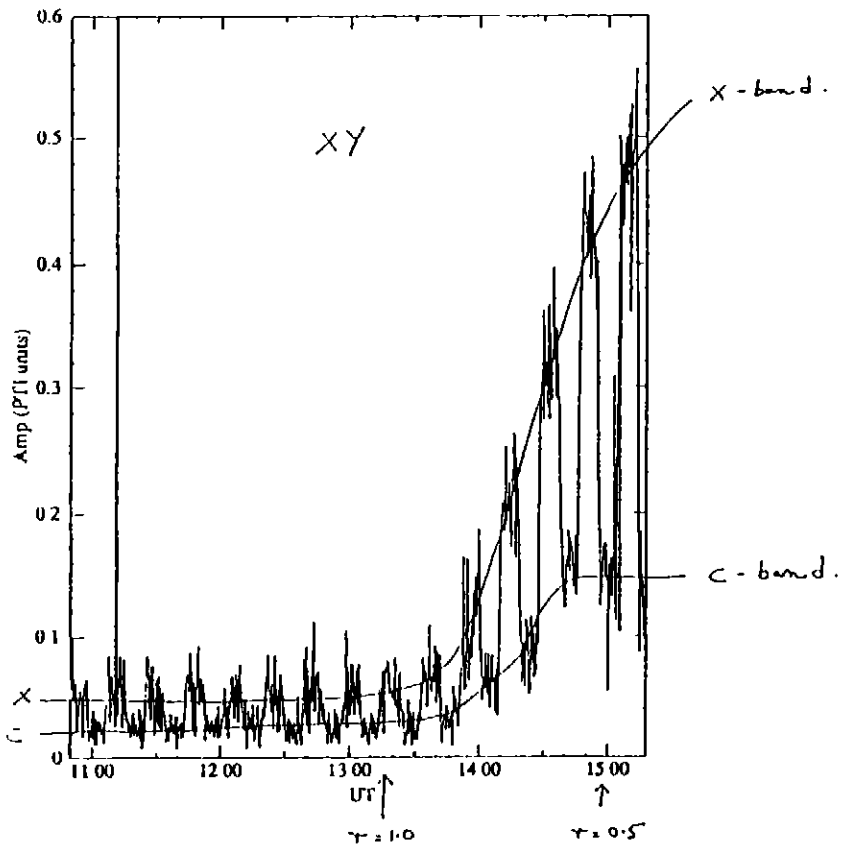

file : CUL2:[RSUBRAHM.ATDAT]1048.RPF
Channel id : 8-24 U BA21 buff 3
sources :
1555+001
file : CUL2:[RSUBRAHM.ATDAT]1048.RPF
Plotted on 31-JUL-90 at 11:51:25
Frequency: 4910.00 MHz
See pu$tmp.plt.lis for a statistical summary

Fig 8 (b)

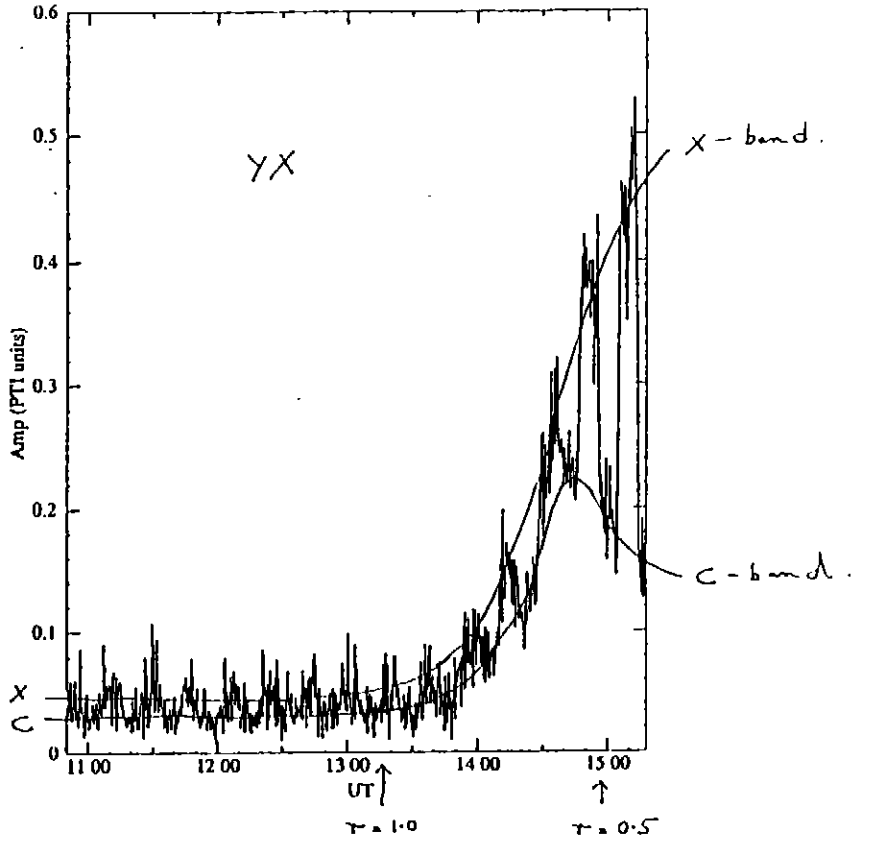

file : CUL2:[RSUBRAHM.ATDAT]1048.RPF
Channel id : 8-24 V BA21 buff 4
sources :
1555+001
file : CUL2:[RSUBRAHM.ATDAT]1048.RPF
Plotted on 31-JUL-90 at 11:51:51
Frequency: 4910.00 MHz
See pu$tmp:plt.lis for a statistical summary

Fig. 9 (a)

L-band.

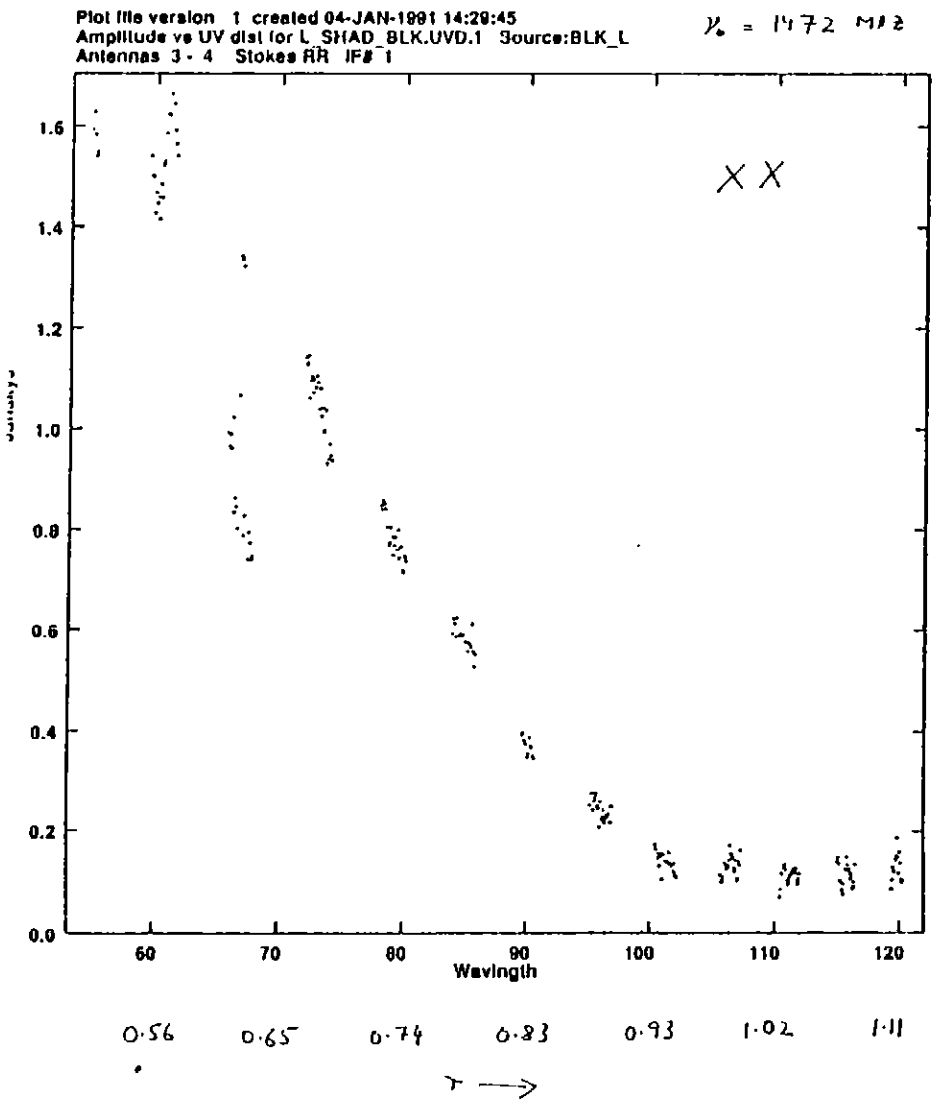

Fig 9 (b)

L-band

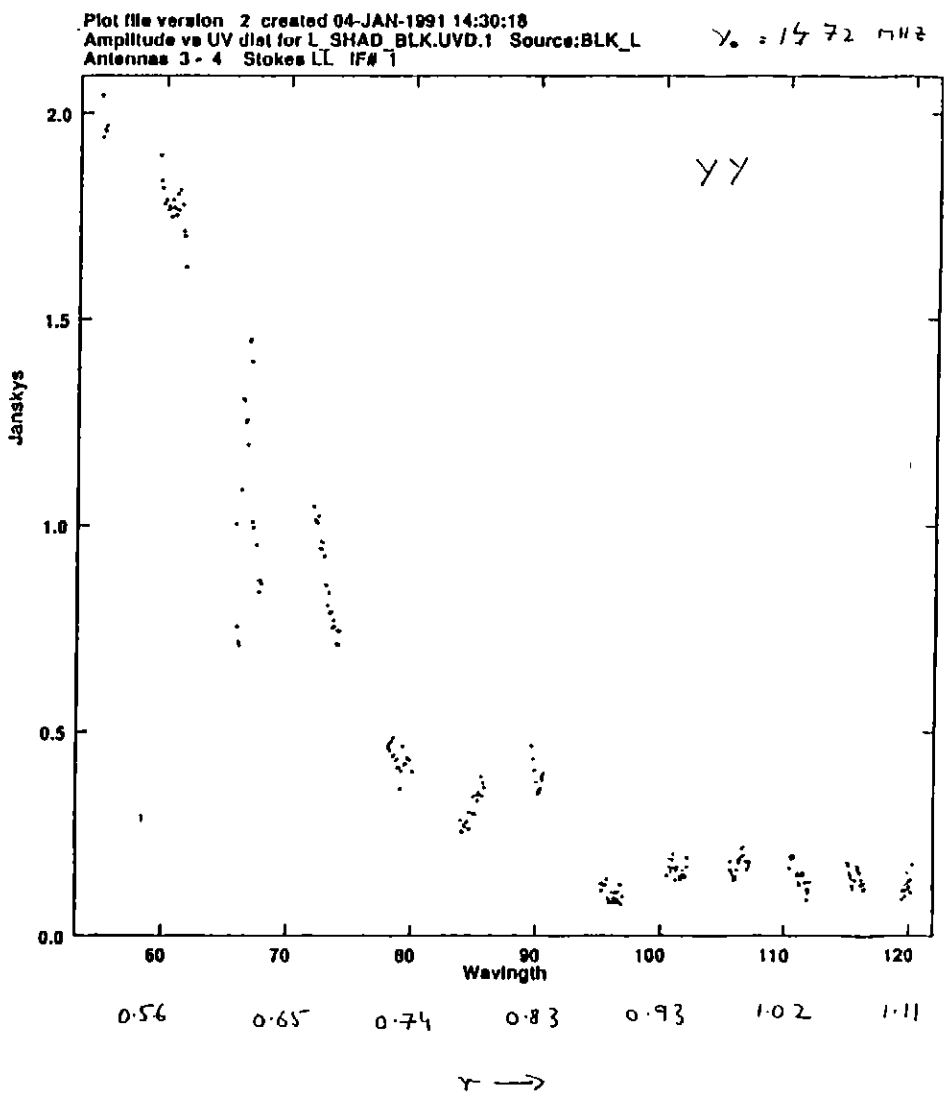

Fig 9 (c)

L - band

ν_0 = 1472 MHz

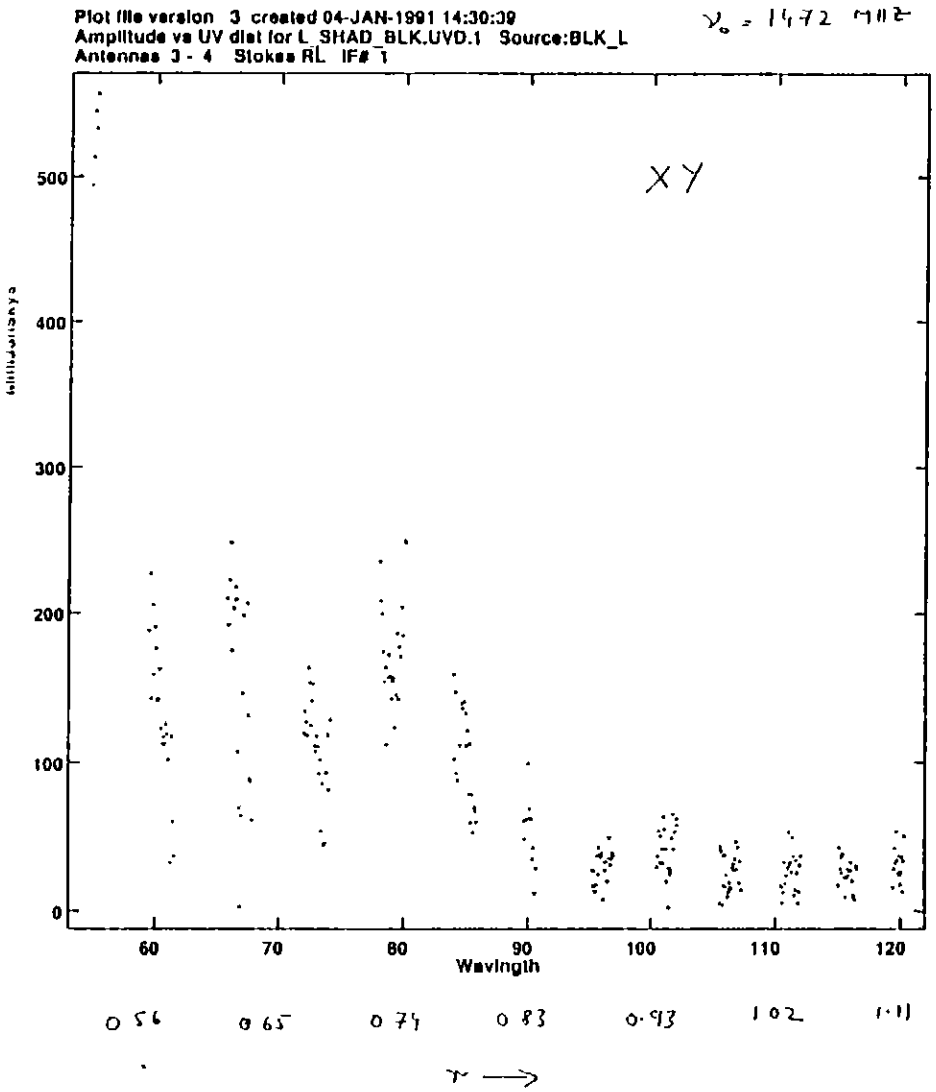

Fig 9 (d)

L - band

ν_0 = 1472 MHz

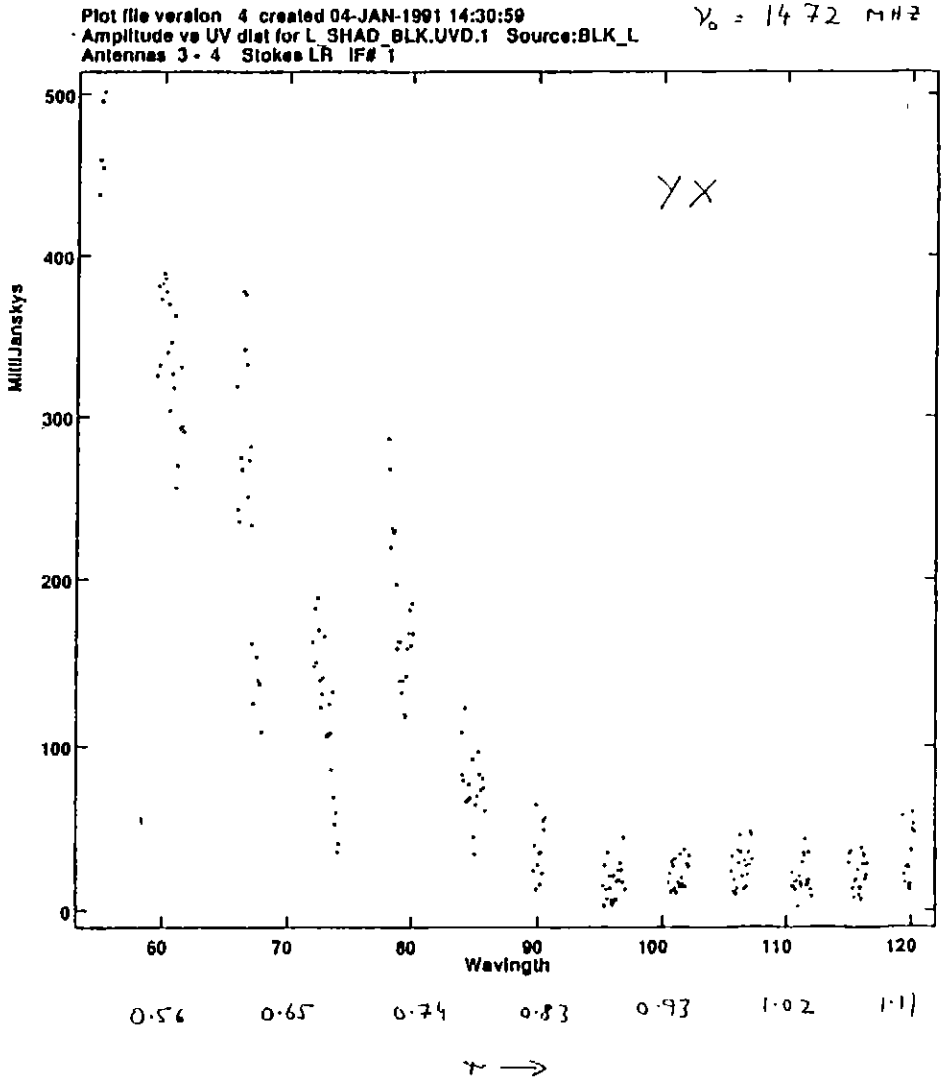

Fig. 10 (a)

S-band

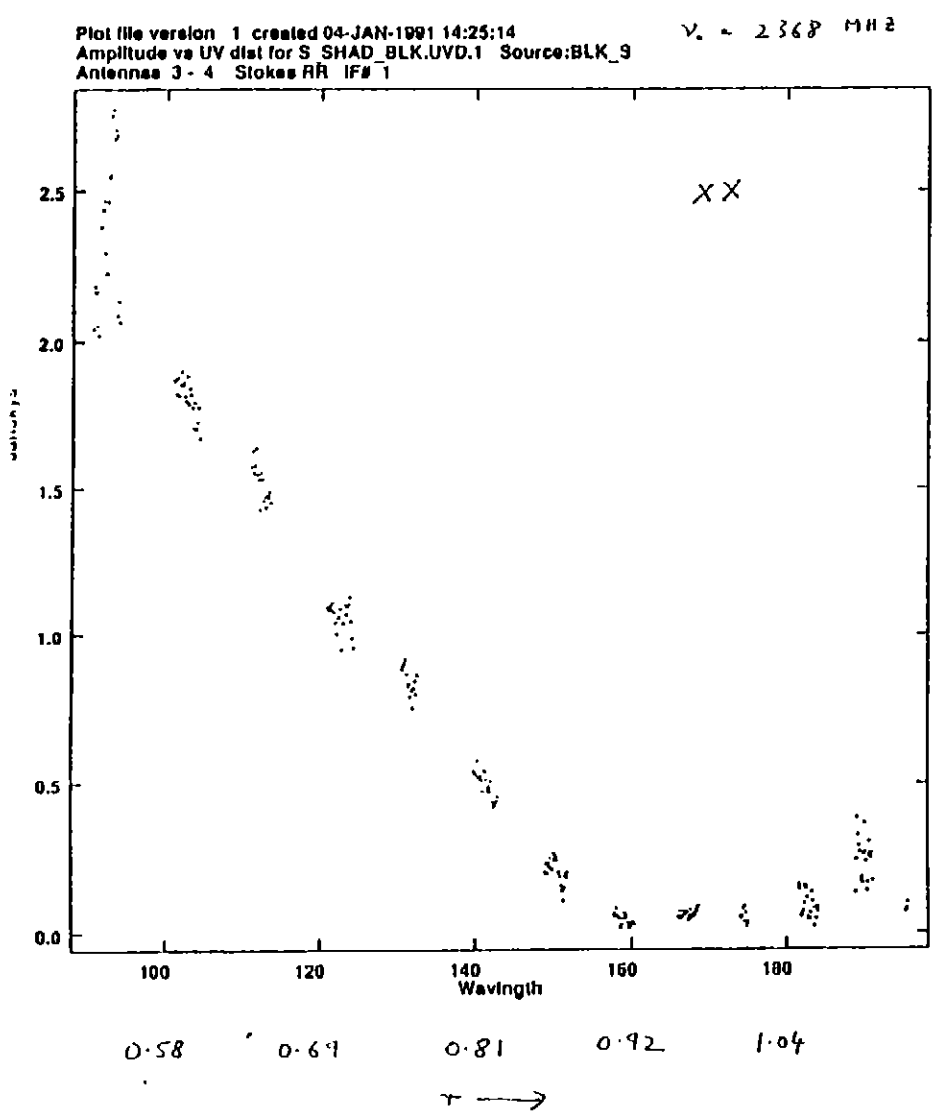

0·58 0·69 0·81 0·92 1·04

τ →

Fig 10 (b)

S-band

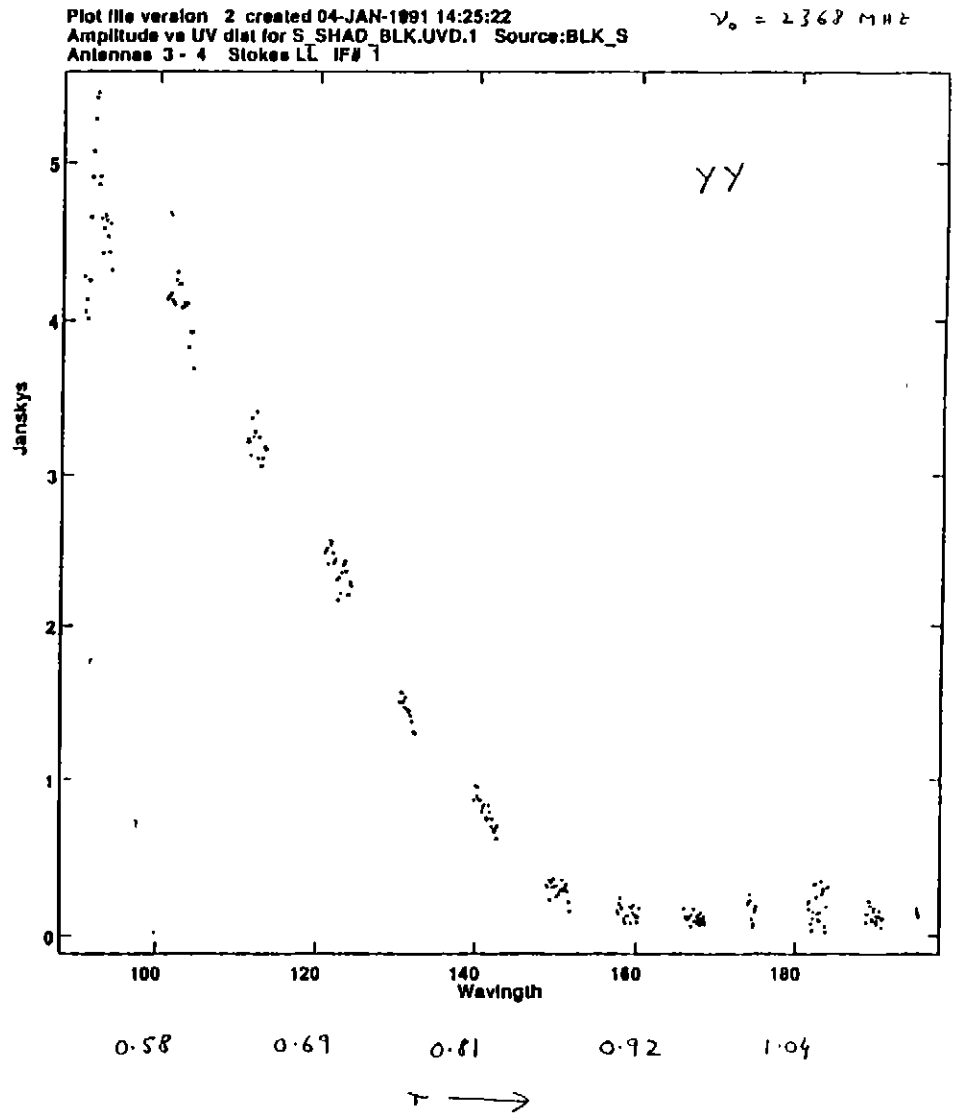

0·58 0·69 0·81 0·92 1·04

τ →

Fig. 10 (c)

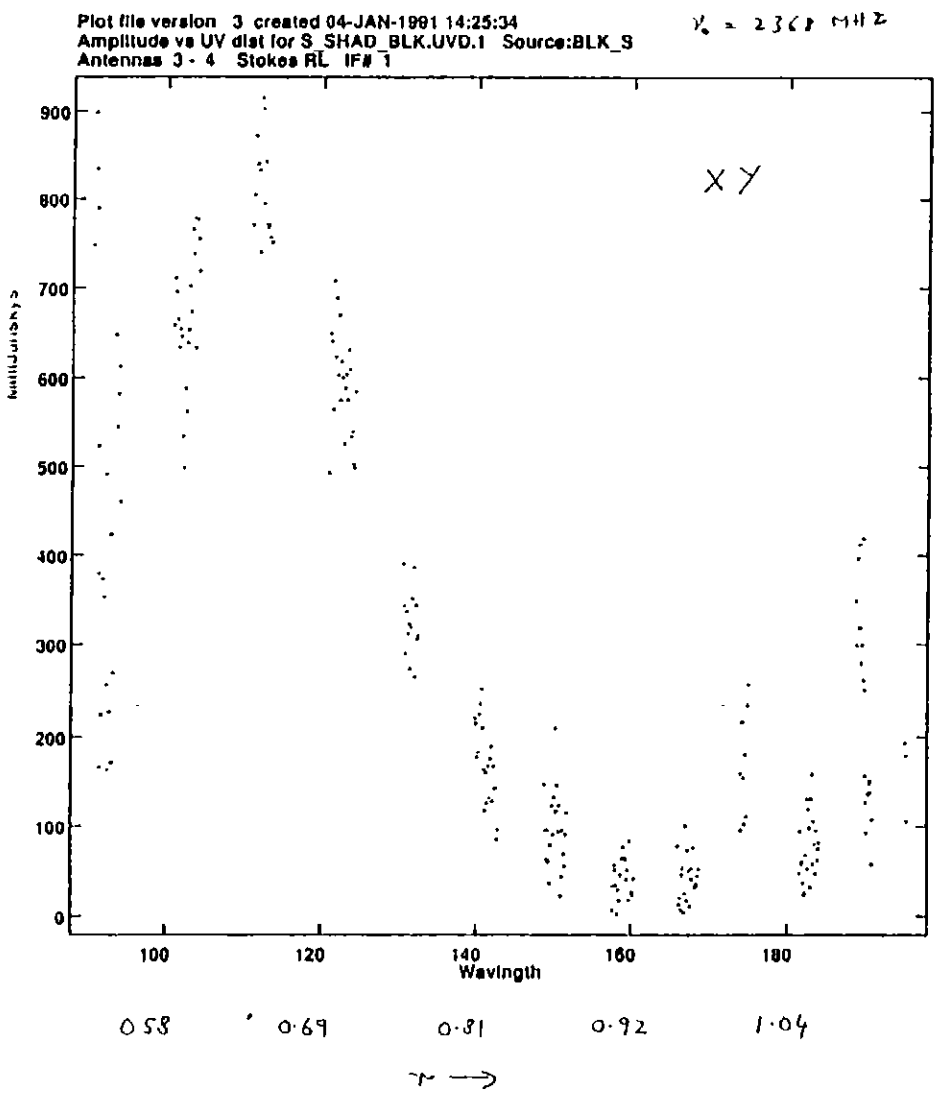

Fig 10 (d)

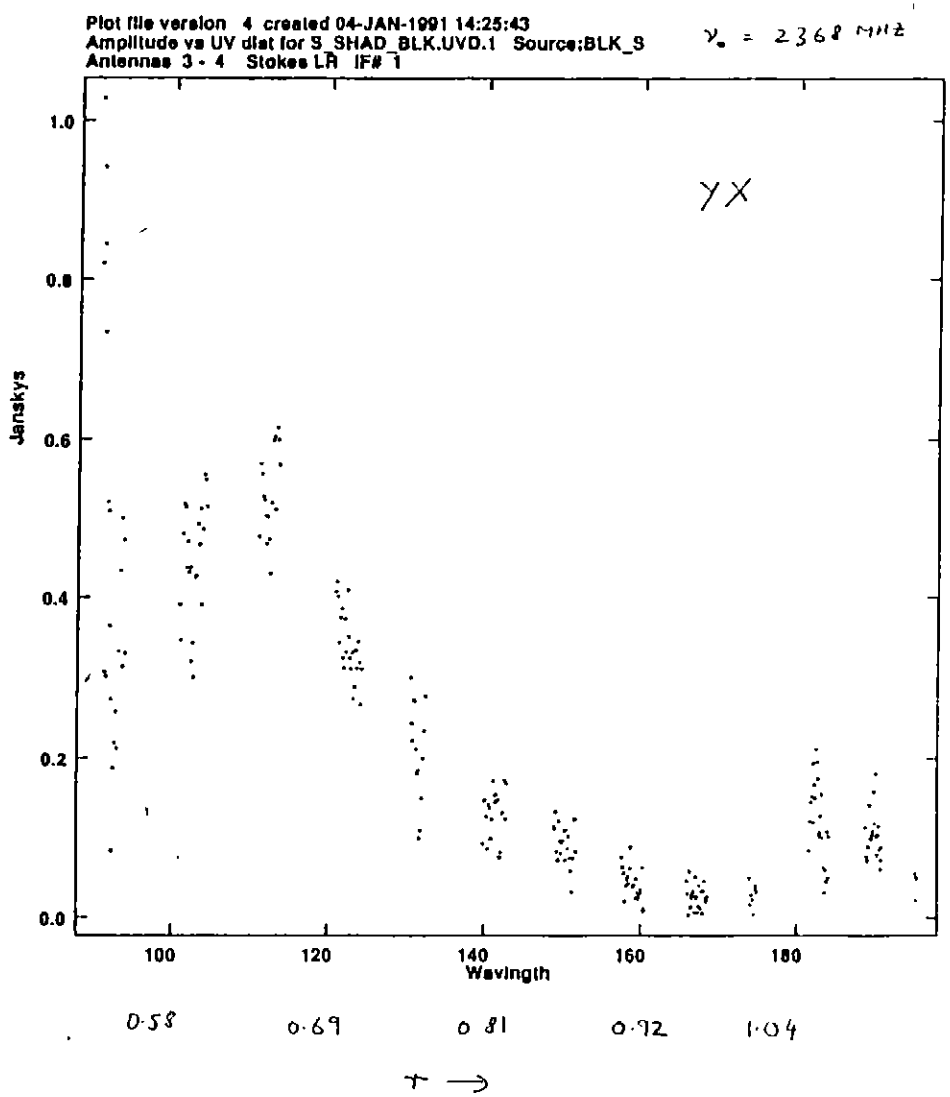

Fig 11 (a)

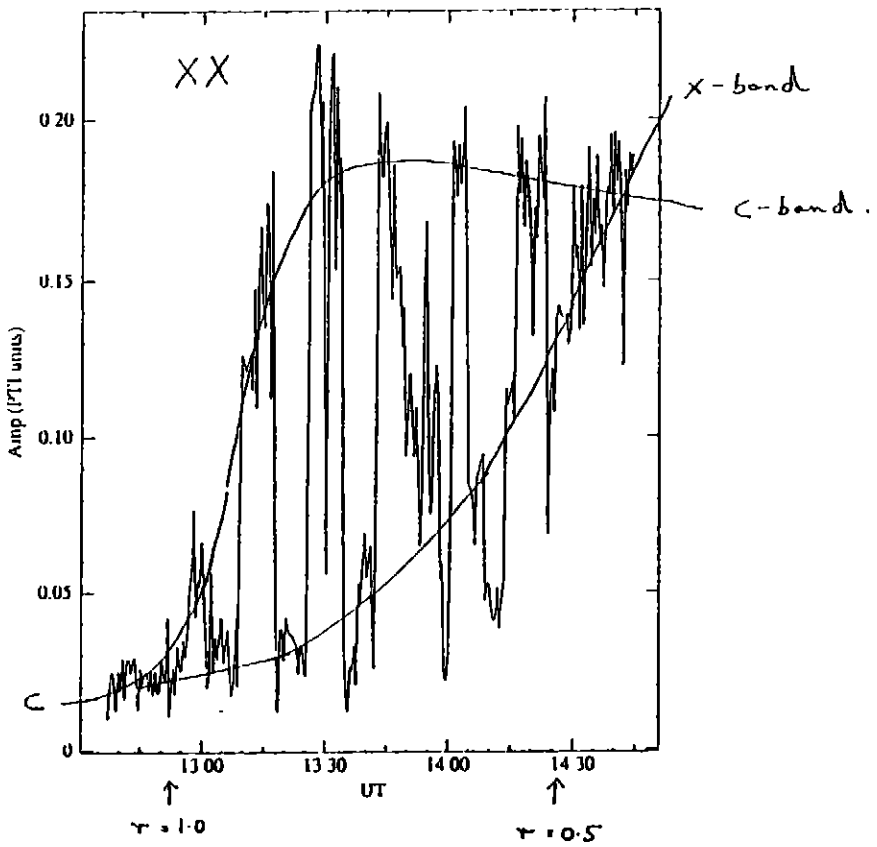

file : CUL2:[OBSERVER DAT]90-08-03_1227.RPF
Channel id : 8-24 I BA12 buff 5
sources :
BLK-C
BLK-X
file : CUL2:[OBSERVER DAT]90 08-03_1227 RPF
Plotted on 7-AUG-90 at 15.03:33
Frequency: 8600.00 MHz
Buffer no: 5 Channel id : 8-24 I BA12

Source Buff		---------- SCALAR ----------					--- VECTOR ---	
Name	No.	npts	mean	rms	max	min	amp	phase
BLK-C	5	41	0.029	0.012	0.051	0.003	0.003	124.3
BLK-X	5	47	0.023	0.012	0.047	0.001	0.001	-55.0
BLK-C	5	47	0.042	0.020	0.099	0.011	0.035	-62.3
BLK-X	5	47	0.031	0.014	0.066	0.010	0.022	-137.6
BLK-C	5	47	0.138	0.037	0.203	0.037	0.129	-86.5
BLK-X	5	47	0.032	0.017	0.073	0.006	0.024	164.9
BLK-C	5	47	0.186	0.051	0.254	0.033	0.125	-119.0
BLK-X	5	47	0.040	0.021	0.087	0.007	0.025	23.5
BLK-C	5	17	0.193	0.027	0.236	0.146	0.192	-112.7
BLK-C	5	110	0.119	0.057	0.223	0.004	0.062	-152.6
BLK-X	5	69	0.071	0.030	0.138	0.014	0.049	-95.1

Fig 11 (b)

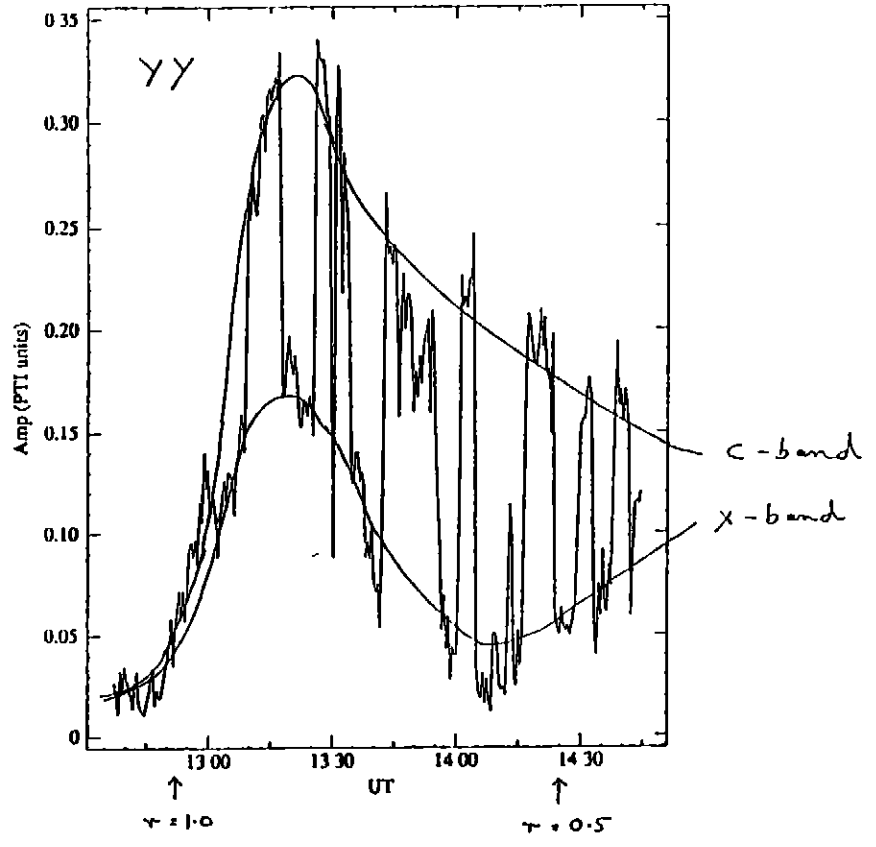

file : CUL2:[OBSERVER.DAT]90-08-03_1227.RPF
Channel id : 8-24 Q BA12 buff 6
sources :
BLK-C
BLK-X
file : CUL2:[OBSERVER.DAT]90 08-03_1227.RPF
Plotted on 7-AUG-90 at 15.03:42
Frequency: 8600.00 MHz
Buffer no: 6 Channel id : 8-24 Q BA12

Source Buff		---------- SCALAR ----------					---- VECTOR ----	
Name	No.	npts	mean	rms	max	min	amp	phase
BLK-C	6	41	0.025	0.011	0.050	0.005	0.011	-172.4
BLK-X	6	47	0.029	0.015	0.066	0.002	0.015	99.6
BLK-C	6	47	0.094	0.031	0.154	0.024	0.091	120.2
BLK-X	6	47	0.125	0.022	0.189	0.084	0.124	57.7
BLK-C	6	47	0.293	0.028	0.353	0.236	0.291	84.3
BLK-X	6	47	0.171	0.018	0.202	0.136	0.170	26.6
BLK-C	6	47	0.277	0.081	0.375	0.065	0.187	33.1
BLK-X	6	47	0.104	0.031	0.169	0.025	0.057	-12.8
BLK-C	6	17	0.243	0.017	0.277	0.213	0.242	16.6
BLK-C	6	110	0.157	0.074	0.259	0.015	0.062	-27.0
BLK-X	6	69	0.038	0.030	0.138	0.002	0.019	-27.7

Fig. 11 (c)

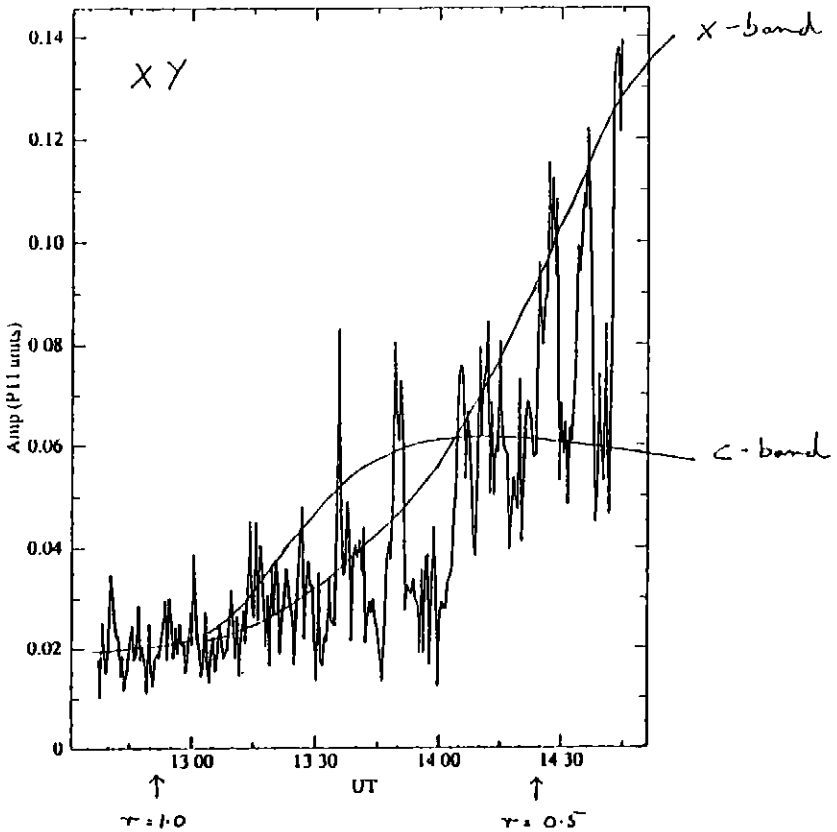

file : CUL2:[OBSERVER.DAT]90-08-03_1227.RPF
Channel id : 8-24 U BA12 buff 7
sources :
BLK_C
BLK_X
file : CUL2:[OBSERVER.DAT]90-08-03_1227.RPF
Plotted on 7-AUG-90 at 15:03:50
Frequency: 8600.00 MHz
Buffer no: 7 Channel id : 8-24 U BA12

Source	Buff	SCALAR					VECTOR	
Name	No.	npts	mean	rms	max	min	amp	phase
BLK_C	7	41	0.021	0.010	0.049	0.006	0.004	25.4
BLK_X	7	47	0.019	0.010	0.045	0.002	0.005	-147.5
BLK_C	7	47	0.023	0.010	0.051	0.003	0.002	-65.3
BLK_X	7	47	0.019	0.011	0.042	0.003	0.004	50.7
BLK_C	7	47	0.029	0.015	0.069	0.007	0.022	167.3
BLK_X	7	47	0.028	0.012	0.066	0.006	0.011	37.2
BLK_C	7	47	0.028	0.014	0.067	0.003	0.019	135.6
BLK_X	7	47	0.041	0.023	0.156	0.010	0.029	90.5
BLK_C	7	17	0.026	0.009	0.045	0.012	0.008	166.8
BLK_C	7	110	0.037	0.019	0.096	0.006	0.010	128.0
BLK_X	7	69	0.063	0.018	0.118	0.026	0.050	-68.7

Fig 11 (d)

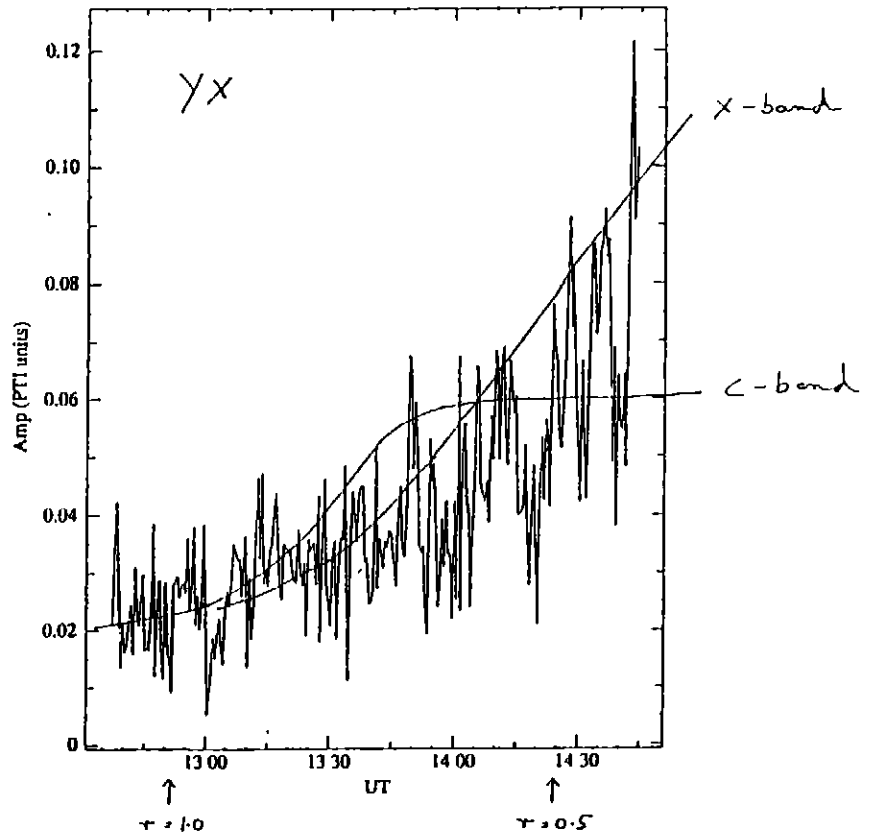

file : CUL2:[OBSERVER.DAT]90-08-03_1227.RPF
Channel id : 8-24 V BA12 buff 8
sources :
BLK_C
BLK_X
file : CUL2:[OBSERVER.DAT]90-08-03_1227.RPF
Plotted on 7-AUG-90 at 15:03:59
Frequency: 8600.00 MHz
Buffer no: 8 Channel id : 8-24 V BA12

Source	Buff	SCALAR					VECTOR	
Name	No.	npts	mean	rms	max	min	amp	phase
BLK_C	8	41	0.024	0.014	0.075	0.002	0.003	179.1
BLK_X	8	47	0.020	0.013	0.059	0.004	0.001	-125.8
BLK_C	8	47	0.027	0.013	0.056	0.004	0.002	-95.5
BLK_X	8	47	0.024	0.013	0.051	0.002	0.013	-169.0
BLK_C	8	47	0.033	0.013	0.069	0.010	0.026	21.8
BLK_X	8	47	0.031	0.011	0.050	0.009	0.023	175.1
BLK_C	8	47	0.032	0.014	0.061	0.004	0.021	28.0
BLK_X	8	47	0.035	0.017	0.077	0.006	0.019	-150.4
BLK_C	8	17	0.035	0.013	0.063	0.007	0.025	19.0
BLK_C	8	110	0.040	0.018	0.086	0.006	0.022	-2.2
BLK_X	8	69	0.054	0.016	0.094	0.024	0.040	58.9

broad band and its uncalibrated visibility phase is not always the same as that of the phase of the source signal.

Although the switched demodulator outputs did not significantly change with decreasing elevation angle, the total power increased as the antennas were tipped to the horizon. The inferred rise in the system temperature was about 90% in the shadowed antenna and 40% in the other antenna as the antennas reached the elevation of 15 degrees.

The XY auto-correlations in the antennas showed 50-100% systematic changes on pointing towards the horizon elevation limit indicating that a significant (>5%) fraction of the increased noise entering the feeds (from the atmosphere/ground) was linearly polarized.

The observations were verified on a different source close to 0 degrees declination and using different centre frequencies in the bands.

Experiments on blank fields : In order to determine the origin of the spurious correlation in shadowed antennas, observations were made on blank fields (at 0 deg. declination) with a pair of 30m spaced antennas over hour angles where the shadowing parameter r reduced from a value above unity down to about 0.5.

L-band : The observed visibility amplitudes in the XX, YY, XY & YX cross-correlations are displayed in Fig. 9 as a function of the shadowing parameter r. Spurious correlated flux density is seen in all four cross-products for $r<1$. The level of the signal is 1-2 Jy in XX & YY and about 0.5 Jy in XY & YX at $r=0.5$.

S-band : The observed amplitudes on all four cross-products are shown as a function of the shadowing parameter r in Fig. 10. With the sensitivity in the 10s averaged visibility, spurious correlation is obviously present even for $r=0.9$ and becomes as much as 2-5 Jy in XX & YY and 0.5-1 Jy in XY & YX products at $r=0.5$.

C/X-bands : Fig. 11 shows the amplitudes on all the four cross-products resulting from observing a blank field alternately with C & X band frequencies. The amplitudes are plotted against time and $r=1$ at 1250 UT and $r=0.5$ at 1425 UT. These observations are not corrected for system temperature variations and the amplitudes should be scaled up by about a factor 5 to obtain a scale in Jy. In both the bands, spurious correlation with a high percentage linear polarization appears for $r<1.0$. The spurious signal is broad band.

Discussion : On observing a source, spurious correlation is seen to appear in the baselines where one antenna shadows the other. The spurious correlation appears even on a blank field suggesting that it does not arise due to a scattering of the source radiation (the effect is additive, not multiplicative). An experiment where the delay tracking centre was well removed from the antenna pointing centre caused the spurious signal to appear in a channel in the lag domain corresponding to a source in the direction that the antennas were pointed. When the pointing of either of the two antennas forming the 30m spacing was offset in azimuth or elevation, the amplitude of the spurious signal dropped. The rate of amplitude fall-off with the offset angle indicated that the effective beam size was 2-3 times the far-field primary beam size. The XY & YX cross-products had a smaller effective beam size as compared to the XX & YY products. Observations in which the calibrator noise sources were turned off in both the antennas forming the 30m spacing were not free of the surious signal.

The experiments suggest that the highly-polarized spurious-signal comes from the near field and from the direction in which the antennas are pointed. This indicates that the signal originates in atmospheric emission. In none of the bands is the signal seen for $r>1$. This indicates that overlap is important and that the correlation arises due to porosity of the antenna surfaces. It may be noted here that such a correlated response to atmospheric emission can arise even if the emission is uniform and without any patchiness because porosity results in zero baselines. A porous antenna is like a partially silvered mirror. If the porosity were in the form of slits, this could also explain the strong polarization in the correlated signal. The system temperature in an antenna was seen to rise by aout 20 deg. when tipped to the horizon elevation limit. In order to produce a cross-correlation at the level of 1 Jy, leakage of -45 dB of this power is sufficient.

Conclusions :

(a) The short 30/60 m baselines are not usable in the hour angle/declination ranges where the shadowing parameter $r<1$, but there appears to be no problem with their use outside this range. The effects of solar interference has not been examined.

(2) Longer baselines containing shadowed antennas could be useful with appropriate corrections. Quantitatively useful corrections can be experimentally determined once the system temperature correction machinery works well.